Joint Pilot Allocation and Robust Beam-vector Design for Ultra-Dense TDD C-RAN

Cunhua Pan*, Hani Mehrpouyan†, Yuanwei Liu‡, Maged Elkashlan*, and Arumugam Nallanathan*
* Queen Mary University of London, London, UK
† Boise State University, Boise, USA
‡ King's College London, London, UK

***Abstract*—This paper deals with the unavailability of full CSI in ultra-dense user-centric TDD C-RAN. To reduce the channel training overhead, we consider the incomplete CSI case, where only large-scale inter-cluster CSI is available. Channel estimation for intra-cluster CSI is also considered, where we formulate a joint pilot allocation and user equipment (UE) selection problem to maximize the number of admitted UEs with fixed number of pilots. A novel pilot allocation algorithm is proposed by considering the multi-UE pilot interference. Then, we consider robust beam-vector optimization problem subject to UEs' data rate requirements and fronthaul capacity constraints, where the channel estimation error and incomplete inter-cluster CSI are considered. Simulation results demonstrate its superiority over the existing algorithms.**

I. Introduction

C-RAN is a promising network architecture that can provide high spectral efficiency and good coverage [1]. The key feature of C-RAN is that the baseband signal processing can be migrated to the baseband unit (BBU) pool so that radio remote heads (RRHs) are only responsible for simple transmission and reception. Due to their simple functionalities, RRHs can be densely deployed to provide ubiquitous service access for a large number of UEs in hot spots. Unlike the conventional ultra-dense small-cell networks where cochannel interference (CCI) is a limiting factor [2], centralized signal processing such as CoMP technique can be adopted in ultra-dense C-RAN to effectively mitigate the CCI.

Recently, transmission design has been extensively studied to deal with various technical issues in conventional C-RAN [3]–[5]. However, the most troublesome challenge is that dense C-RAN requires large amount of CSI that is needed by dense C-RAN to facilitate centralized signal processing. The acquisition of these CSI requires large amount of training overhead that increases with the network size. Results in [6] showed that the network performance may even decrease with increasing number of RRHs when taking into account the cost of acquiring CSI. One promising way to reduce the training overhead is to consider the incomplete CSI case, where each UE only measures its CSI from the RRHs in its serving cluster (named intra-cluster CSI) and only tracks the large-scale fading (path loss and shadowing) for the CSI outside its cluster (named inter-cluster CSI). Recently, transmission design considering the incomplete CSI has attracted research interests [7]–[9].

However, intra-cluster CSI was assumed to be perfectly known in [7]–[9], which is impractical for dense C-RAN. To estimate the intra-cluster CSI in TDD C-RAN, the uplink training pilot sequences sent from the UEs that share at least one serving RRH should be mutually orthogonal so that the BBU pool can differentiate the CSI of the shared RRH to the corresponding UEs. One naive method is to assign all the UEs with mutually orthogonal pilot sequences. However, the number of time slots required for training will increase linearly with the number of UEs, which is unaffordable for ultra-dense C-RAN. Hence, one should allow some UEs to reuse the same pilots. The pilot reuse scheme will incur the pilot contamination issue, which results in sizeable channel estimation error that should be taken into account when designing beam-vectors. Hence, in this paper, we consider both the channel estimation procedure of intra-cluster CSI and the robust beam-vector design.

Hence, in this paper, we consider a two-stage optimization problem for dense C-RAN, i.e., channel estimation for intra-cluster CSI in Stage I and robust beam-vector design in Stage II. Specifically, In Stage I, we formulate a joint UE selection and pilot allocation problem to maximize the number of admitted UEs with fixed number of available pilots. A novel pilot allocation algorithm is proposed by considering the multi-UE pilot interference; Based on the results from Stage I, in Stage II beam-vectors are designed to minimize the transmit power based on the imperfect intra-cluster CSI and incomplete inter-cluster CSI. Both UEs' data rate and fronthaul capacity constraints are considered.

Notations: For a set $\mathcal{A}$, $|\mathcal{A}|$ is the cardinality of $\mathcal{A}$. The complex Gaussian distribution is denoted as $\mathcal{CN}(\cdot,\cdot)$ and $\mathbb{C}$ is used to represent the complex set. The lower-case bold letters means vectors and upper-case bold letters denote matrices.

II. System Model

A. Signal Transmission Model

Consider a downlink dense TDD C-RAN with I RRHs and K UEs in Fig. 1. Each RRH and each UE have M antennas and a single antenna, respectively. Denote the set of RRHs and UEs as $\mathcal{I}$ and $\bar{\mathcal{U}}$, respectively. Each RRH is connected to the BBU pool through the fronthaul links. The BBU pool is assumed to have all UEs' data and send each UE's data to a carefully selected set of RRHs through the fronthaul links.

The set of UEs that are admitted is denoted by $\mathcal{U} \subseteq \bar{\mathcal{U}}$. The user-centric cluster is adopted to reduce the computational complexity where each UE is only served by its nearby RRHs.

978-1-5090-5019-2/17/$31.00 ©2017 IEEE

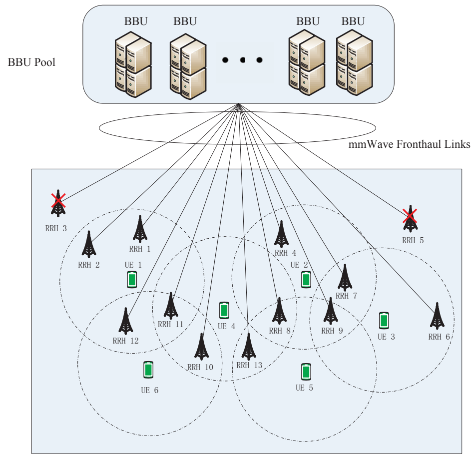

Fig. 1. Illustration of a user-centric C-RAN where each UE is served by the RRHs within the dashed circle centered at itself.

Denote $\mathcal{I}_k \subseteq \mathcal{I}$ and $\mathcal{U}_i \subseteq \mathcal{U}$ as the set of RRHs that potentially serve UE k and the set of UEs that are potentially served by RRH i, respectively. The clusters are assumed to be fixed as they are formed based on long term CSI [9].

Denote $\mathbf{h}_{i,k} \in \mathbb{C}^{M\times 1}$ and $\mathbf{w}_{i,k} \in \mathbb{C}^{M\times 1}$ as the channel vector and the beam-vector from RRH i to UE k, respectively. Then, the baseband received signal at UE k is given by

$$y_k = \underbrace{\sum\nolimits_{i\in\mathcal{I}_k} \mathbf{h}_{i,k}^{\mathrm{H}}\mathbf{w}_{i,k}s_k}_{\text{desired signal}} + \underbrace{\sum\nolimits_{l\neq k, l\in\mathcal{U}} \sum\nolimits_{i\in\mathcal{I}_l} \mathbf{h}_{i,k}^{\mathrm{H}}\mathbf{w}_{i,l}s_l}_{\text{interference}} + z_k, \tag{1}$$

where s_k is the data symbol for UE k, z_k is the additive complex white Gaussian noise following the distribution of $\mathcal{CN}(0,\sigma_k^2)$. It is assumed that $\mathbb{E}\{|s_k|^2\} = 1$ and $\mathbb{E}\{s_{k_1}s_{k_2}\} = 0$ for $k_1 \neq k_2, \forall k_1, k_2 \in \mathcal{U}$. The channel vector $\mathbf{h}_{i,k}$ can be decomposed as $\mathbf{h}_{i,k} = \sqrt{\alpha_{i,k}}\bar{\mathbf{h}}_{i,k}$, where $\alpha_{i,k}$ denotes the large-scale channel gain that includes the path loss and shadowing, and $\bar{\mathbf{h}}_{i,k}$ denotes the small-scale fading following the distribution of $\mathcal{CN}(\mathbf{0},\mathbf{I})$.

B. Channel Estimation for Intra-cluster CSI

We assume that each UE k only measures the CSI to the RRHs in its cluster $\mathcal{I}_k$, while the BBU pool only knows the large-scale channel gains for the inter-cluster CSI.

In this paper, we assume that τ time slots are used for channel training that satisfies $\tau < K$. Denote the available pilot set as $\mathcal{Q} = \{1, 2, \cdots, \tau\}$, and the orthogonal pilot sequences as $\mathbf{Q} = [\mathbf{q}_1, \cdots, \mathbf{q}_\tau] \in \mathbb{C}^{\tau\times\tau}$. Denote an arbitrary pilot reuse scheme as $\mathcal{P}(\mathcal{U},\mathcal{Q}) = \{(k,\pi_k) : k \in \mathcal{U}, \pi_k \in \mathcal{Q}\}$, where (k,π_k) denotes that UE k is allocated with pilot sequence $\mathbf{q}_{\pi_k}$. In addition, define $\mathcal{K}_\pi = \{k : \pi_k = \pi\}$ as the set of UEs that reuse the πth pilot sequences.

Given the pilot reuse scheme $\mathcal{P}(\mathcal{U},\mathcal{Q})$, the MMSE estimate of channel $\mathbf{h}_{i,k}$ is given by

$$\hat{\mathbf{h}}_{i,k} = \frac{\alpha_{i,k}}{\sum_{l\in\mathcal{K}_{\pi_k}} \alpha_{i,l} + \hat{\sigma}^2}\left(\sum_{l\in\mathcal{K}_{\pi_k}} \mathbf{h}_{i,l} + \mathbf{n}_i\right), \tag{2}$$

where $\mathbf{n}_i \in \mathbb{C}^{M\times 1}$ is the noise vector whose elements are independently generated and follow the distributions of $\mathcal{CN}(0,\sigma^2)$, $\hat{\sigma}^2 = \sigma^2/p_t$ and p_t is the pilot transmit power. The channel estimation error $\tilde{\mathbf{h}}_{i,k} = \mathbf{h}_{i,k} - \hat{\mathbf{h}}_{i,k}$ is independently distributed as $\mathcal{CN}(\mathbf{0},\delta_{i,k}\mathbf{I})$, where $\delta_{i,k}$ is

$$\delta_{i,k} = \frac{\alpha_{i,k}\left(\sum_{l\in\mathcal{K}_{\pi_k}\setminus\{k\}} \alpha_{i,l} + \hat{\sigma}^2\right)}{\sum_{l\in\mathcal{K}_{\pi_k}} \alpha_{i,l} + \hat{\sigma}^2}. \tag{3}$$

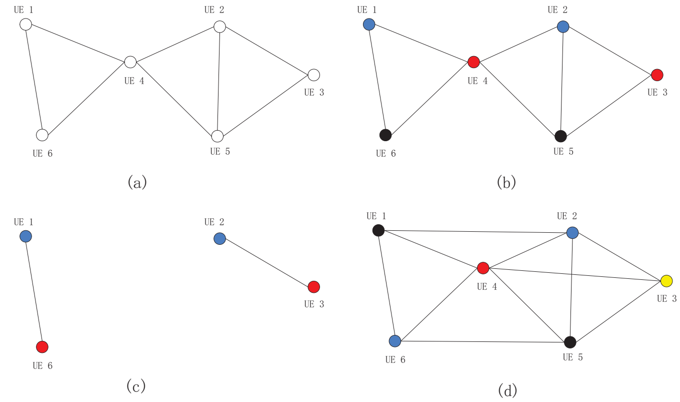

Fig. 2. (a) Construction of the undirected graph for the network in Fig. 1, where any two UEs sharing at least one RRH should be connected; (b) The colored graph after applying the Dsatur algorithm with $n_{\max} = 2$, the minimum number of pilots required is $n^* = 3$. (c) The UE selection and pilot reallocation result after applying Algorithm 1 when $\tau = 2$ and $n_{\max} = 2$, the number of selected UEs is four; (d) The pilot reallocation result after applying Algorithm 2 when $\tau = 4$ and $n_{\max} = 2$. In this colored graph, UE 1 and UE 2 use different pilots to avoid the pilot interference, and the same holds for UE 5 and UE6. In addition, UE 3 and UE 4 are allocated with different pilots, which additionally reduces the pilot interference.

III. Stage I: Pilot Allocation and UE Selection

In dense C-RAN, the UEs served by the same RRH should be allocated with orthogonal training sequences:

$$\mathrm{C1}: \mathbf{q}_{\pi_k}^{\mathrm{H}}\mathbf{q}_{\pi_{k'}'} = 0, \text{for } k, k' \in \mathcal{U}_i, k \neq k', \forall i \in \mathcal{I}.$$

Second, to reduce the channel estimation error, the reuse times for each pilot sequence should be restricted under a predefined value. Denote the number of UEs that share pilot l as n_l, then the constraints can be expressed as

$$\mathrm{C2}: n_l \leq n_{\max}, \forall l \in \mathcal{Q}.$$

In Stage I, we aim to find the maximum number of admitted UEs with a fixed number of pilots, which is formulated as

$$\mathcal{P}_1: \max_{\mathcal{U}\subseteq\bar{\mathcal{U}},\mathcal{P}(\mathcal{U},\mathcal{Q})} \quad |\mathcal{U}|$$
$$\text{s.t.} \quad \mathrm{C1}, \mathrm{C2}.$$

The optimal solution of Problem $\mathcal{P}_1$ can be obtained by the exhaustive search method, and its complexity increases exponentially with K, which is not practical for dense C-RAN. In the following, we provide one low-complexity scheme.

Constraints C1 can be represented by a $K\times K$ binary matrix $\mathbf{B}$, where each element is

$$b_{k,k'} = \begin{cases} 1, & \text{if } \mathcal{I}_k \cap \mathcal{I}_{k'} \neq \emptyset \text{ and } k \neq k' \\ 0, & \text{otherwise,} \end{cases} \tag{5}$$

where $b_{k,k'}$ denotes the (k,k')th element of matrix $\mathbf{B}$. Based on matrix $\mathbf{B}$, we can construct an undirected graph to describe the relationship between any two UEs for constraint C1. For the network in Fig. 1, the graph is constructed in Fig. 2 (a). The graph coloring algorithm such as the Dsatur algorithm

[10], which aims for coloring the vertexes of a graph with the minimum number of different colors under the same constraints in C1 and C2 for a given set of UEs, has been used in [11] to design the pilot allocation. For the graph in Fig. 2 (a), the final colored graph is shown in Fig. 2 (b) after using the algorithm. However, given the set of pilots, how to design the pilot allocation scheme to maximize the number of admitted UEs needs further investigation.

To resolve this issue, we first adopt the Dsatur algorithm to find the minimum number of colors that are required. If the number is larger than the number of available pilots, some UEs should be removed. Otherwise, all UEs can be admitted. For the latter case, the pilot allocation results may be that some pilots have not been allocated while some pilots are reused by many users, which wastes the pilot resources. In this case, we can reallocate all of the available pilots to the UEs to reduce the pilot contamination. The details of each case will be discussed in the following.

Denote the minimum number of pilots required as n^*. In the following, we discuss two cases: 1) $n^* > \tau$; 2) $n^* < \tau$ [1].

Case I: $n^* > \tau$. In this case, some UEs should be removed. Define $\theta_k \triangleq \sum_{k'\neq k, k'\in\bar{\mathcal{U}}} b_{k,k'}$ as the total number of different UEs to which UE k is connected to. In general, the UE with the largest θ_k should be removed since many UEs should use different pilots from that used by the UE. However, there are some cases that different UEs has the same largest θ_k, and randomly removing one UE may incur inferior performance. Intuitively, the UE that incurs the highest pilot contamination should be removed. To this end, we first define a metric $\eta_{k,k'}$ to measure the level of pilot contamination between any two unconnected UEs when they are allocated with the same pilot,

$$\eta_{k,k'} = \log\left(1+\frac{\sum_{i\in\mathcal{I}_{k'}}\alpha_{i,k}}{\sum_{i\in\mathcal{I}_k}\alpha_{i,k}}\right)+\log\left(1+\frac{\sum_{i\in\mathcal{I}_k}\alpha_{i,k'}}{\sum_{i\in\mathcal{I}_{k'}}\alpha_{i,k'}}\right). \quad (6)$$

Obviously, larger $\eta_{k,k'}$ means more severe pilot contamination between UE k and UE k'. Then, define $\xi_k = \sum_{k'\in\mathcal{K}_{\pi_k}\setminus\{k\}}\eta_{k,k'}$ as the value to measure the level of pilot contamination when keeping UE k. Then, the UE with the largest value of ξ_k should be removed.

Based on this idea, we provide a UE selection and pilot reallocation algorithm in Algorithm 1. By using this algorithm to the network in Fig. 1, the result is shown in Fig. 2 c).

Algorithm 1 UE selection and pilot reallocation for Case I

1: Initialize the matrix $\mathbf{B}$, the UE set $\mathcal{U}=\bar{\mathcal{U}}=\{1,\cdots,K\}$, the initial number of required pilots n^* from the Dsatur algorithm;
2: While $n^* > \tau$
3: Find $k^* = \arg\max_{k\in\mathcal{U}}\theta_k$. If there are two UEs with the same values of θ_k, remove the UE with the largest ξ_k;
4: Remove UE k^* from $\mathcal{U}$, i.e., $\mathcal{U}$=$\mathcal{U}/k^*$, and update matrix $\mathbf{B}$ with current $\mathcal{U}$;
5: Use Dsatur algorithm to calculate n^* with $\mathbf{B}$ and $\mathcal{U}$;

[1]No operation is required for $n^* = \tau$.

Case II: $n^* < \tau$. In this case, only part of the pilots are allocated. To reduce the pilot contamination, all the available pilots should be allocated to UEs. For example, in Fig. 2 b) with three allocated pilots, there may exist measurable pilot interference between UE 1 and UE 2 since they are not so far. When there are four available pilots, the pilots can be reallocated to resolve this issue. For example, in Fig. 2 d), UE 1 and UE 2 are able to be allocated with different pilots. Hence, the pilot contamination can be additionally mitigated.

According to the definition of $\eta_{k,k'}$ in (6), the pair of UEs with larger $\eta_{k,k'}$ should be allocated with different pilots, while for the pair with smaller $\eta_{k,k'}$, they can be allocated with the same pilot. Hence, a threshold $\eta_{\rm th}$ is introduced to reconstruct the undirected graph. Specifically, when $\eta_{k,k'} > \eta_{\rm th}$, no reuse is allowed. Otherwise, they can reuse the same pilot. Hence, the binary matrix $\mathbf{B}$ can be reconstructed as follows

$$b_{k,k'} = \begin{cases} 1, \text{ if } \mathcal{I}_k\cap\mathcal{I}_{k'}\neq\emptyset \text{ and } k\neq k', \\ 1, \text{ if } \eta_{k,k'}>\eta_{\rm th},\ \mathcal{I}_k\cap\mathcal{I}_{k'}=\emptyset\ \ k\neq k', \\ 0, \text{ otherwise}. \end{cases} \quad (7)$$

Obviously, when $\eta_{\rm th}$ is small, more UEs will be connected and more pilots are required. In the extreme case when $\eta_{\rm th} < \min\{\eta_{k,k'}\}$, all UEs will be connected with each other and the number of required pilots is equal to K. On the other hand, when $\eta_{\rm th}\geq\max\{\eta_{k,k'}\}$, the reconstructed binary matrix $\mathbf{B}$ in (7) reduces to the conventional binary matrix $\mathbf{B}$ in (5), and the number of required pilots is equal to n^*. As it is assumed that $\tau < K$, there must exist at least one $\eta_{\rm th}$ between $\min\{\eta_{k,k'}\}$ and $\max\{\eta_{k,k'}\}$ that the number of required pilots is equal to τ. As a result, the bisection search method can be adopted to find the $\eta_{\rm th}$ such that the required number of pilots is equal to τ. The details are given in Algorithm 2. Fig. 2 d) shows the pilot allocation results after using Algorithm 2.

Algorithm 2 Pilot reallocation algorithm for Case II

1: Initialize $\eta_{\rm th,L} = \min\{b_{k,k'}\}$, $\eta_{\rm th,U} = \max\{b_{k,k'}\}$, the initial number n^* from the Dsatur algorithm;
2: While $n^*\neq\tau$
3: Set $\eta_{\rm th} = (\eta_{\rm th,L}+\eta_{\rm th,U})/2$, update the binary matrix $\mathbf{B}$ in (7). Use the Dsatur algorithm to calculate n^*.
4: If $n^* > \tau$, set $\eta_{\rm th,L} = \eta_{\rm th}$; If $n^* < \tau$, set $\eta_{\rm th,U} = \eta_{\rm th}$;

IV. Stage II: Robust Beamforming Design

Denote the set of UEs selected from Stage I as $\widetilde{\mathcal{U}}$. The beamvectors for each UE are merged into a single large-dimension vector $\mathbf{w}_k = [\mathbf{w}_{i,k}^{\rm H}, \forall i\in\mathcal{I}_k]^{\rm H}$. Similarly, define a set of new channel vectors $\mathbf{g}_{l,k} = [\mathbf{h}_{i,k}^{\rm H}, \forall i\in\mathcal{I}_l]^{\rm H}$, representing the aggregated perfect CSI from the RRHs in $\mathcal{I}_l$ to UE k. Also, define $\tilde{\mathbf{g}}_{k,k} = [\tilde{\mathbf{h}}_{i,k}^{\rm H}, \forall i\in\mathcal{I}_k]^{\rm H}$ and $\hat{\mathbf{g}}_{k,k} = [\hat{\mathbf{h}}_{i,k}^{\rm H}, \forall i\in\mathcal{I}_k]^{\rm H}$ as the aggregated CSI error and estimated CSI from the RRHs in $\mathcal{I}_k$ to UE k, respectively. Since channel estimation error is expressed as $\tilde{\mathbf{g}}_{k,k} = \mathbf{g}_{k,k} - \hat{\mathbf{g}}_{k,k}$, the received signal model in (1) can be rewritten as

$$y_k = \hat{\mathbf{g}}_{k,k}^{\rm H}\mathbf{w}_k s_k + \tilde{\mathbf{g}}_{k,k}^{\rm H}\mathbf{w}_k s_k + \sum\nolimits_{l\neq k, l\in\mathcal{U}}\mathbf{g}_{l,k}^{\rm H}\mathbf{w}_l s_l + z_k. \quad (8)$$

As in [12], we consider the achievable data rate where the term corresponding to the channel estimation error in (8) is regarded as Gaussian noise. Specifically, the achievable data rate for UE $k \in \tilde{\mathcal{U}}$ is written as

$$r_k = \frac{T-\tau}{T}\mathbb{E}\left\{\log_2\left(1+\frac{\left|\hat{\mathbf{g}}_{k,k}^{\mathrm{H}}\mathbf{w}_k\right|^2}{\left|\tilde{\mathbf{g}}_{k,k}^{\mathrm{H}}\mathbf{w}_k\right|^2+\sum\limits_{l\neq k,l\in\mathcal{U}}\left|\mathbf{g}_{l,k}^{\mathrm{H}}\mathbf{w}_l\right|^2+\sigma_k^2}\right)\right\},$$

where T denotes the coherence time of the channel in terms of time slots, the expectation is taken with respect to the unknown channel estimation errors $\left\{\tilde{\mathbf{h}}_{i,k}, i\in\mathcal{I}_k, \forall k\in\tilde{\mathcal{U}}\right\}$, and the small-scale inter-cluster CSI $\{\mathbf{h}_{i,k}, i\in\mathcal{I}\backslash\mathcal{I}_k\}$. Each UE should have its own rate target $R_{k,\min}$:

$$\mathrm{C3}: r_k \geq R_{k,\min}, \forall k\in\tilde{\mathcal{U}}.$$

Also, each fronthaul link should have its capacity limit:

$$\mathrm{C4}: \sum\nolimits_{k\in\mathcal{U}_i}\varepsilon\left(\|\mathbf{w}_{i,k}\|^2\right) r_k \leq C_{i,\max}, \forall i\in\mathcal{I},$$

where $\varepsilon(\cdot)$ is an indicator function, defined as $\varepsilon(x)=1$ if $x\neq 0$, otherwise, $\varepsilon(x)=0$. $C_{i,\max}$ is the maximum data rate that can be supported by the ith fronthaul link.

Finally, each RRH has its own power constraint, given by

$$\mathrm{C5}: \sum\nolimits_{k\in\mathcal{U}_i}\|\mathbf{w}_{i,k}\|^2 \leq P_{i,\max}, i\in\mathcal{I},$$

where $P_{i,\max}$ is the power constraint of RRH i.

In Stage II, we aim to jointly optimize the UE-RRH associations and beam-vectors to minimize the total transmit power of the dense C-RAN network, while satisfying constraints in C3-C5. Hence, this problem can be formulated as

$$\begin{aligned}\mathcal{P}_2: \min_{\mathbf{w}} \quad & \sum\nolimits_{k\in\tilde{\mathcal{U}}}\sum\nolimits_{i\in\mathcal{I}}\|\mathbf{w}_{i,k}\|^2\\ \text{s.t.} \quad & \mathrm{C3}, \mathrm{C4}, \mathrm{C5},\end{aligned}$$

where $\mathbf{w}$ denotes the collection of all beam-vectors.

The imperfect intra-cluster CSI and incomplete inter-cluster CSI make the accurate closed-form expression of the data rate difficult to obtain. In the following, we first obtain the lower-bound of the data rate and replace it with its lower bound to make the optimization problem more tractable. By using Jensen's inequality, the lower bound of the data rate can be derived as

$$\begin{aligned} r_k \quad &\geq \quad \frac{T-\tau}{T}\log_2\left(1+\frac{\left|\hat{\mathbf{g}}_{k,k}^{\mathrm{H}}\mathbf{w}_k\right|^2}{J_k+\sigma_k^2}\right)\\ &= \frac{T-\tau}{T}\log_2\left(1+\frac{\left|\hat{\mathbf{g}}_{k,k}^{\mathrm{H}}\mathbf{w}_k\right|^2}{\mathbf{w}_k^{\mathrm{H}}\mathbf{E}_{k,k}\mathbf{w}_k+\sum\limits_{l\neq k,l\in\mathcal{U}}\mathbf{w}_l^{\mathrm{H}}\mathbf{A}_{l,k}\mathbf{w}_l+\sigma_k^2}\right)\\ &\triangleq \quad \tilde{r}_k \end{aligned} \tag{9}$$

where $J_k = \mathbb{E}\left\{\left|\tilde{\mathbf{g}}_{k,k}^{\mathrm{H}}\mathbf{w}_k\right|^2\right\}+\sum_{l\neq k,l\in\mathcal{U}}\mathbb{E}\left\{\left|\mathbf{g}_{l,k}^{\mathrm{H}}\mathbf{w}_l\right|^2\right\}$, $\mathbf{E}_{k,k} = \mathrm{blkdiag}\left\{\varepsilon_{i,k}\mathbf{I}_{M\times M}, i\in\mathcal{I}_k\right\}$, and $\mathbf{A}_{l,k} = \mathbb{E}\left\{\mathbf{g}_{l,k}^{\mathrm{H}}\mathbf{g}_{l,k}\right\} \in \mathbb{C}^{M|\mathcal{I}_l|\times M|\mathcal{I}_l|}$. To obtain the expression of $\mathbf{A}_{l,k}$, we define the indices of $\mathcal{I}_l$ as $\mathcal{I}_l=\{s_1^l,\cdots,s_{|\mathcal{I}_l|}^l\}$. Then, we have

$$\mathbf{A}_{l,k}=\begin{bmatrix}(\mathbf{A}_{l,k})_{1,1} & \cdots & (\mathbf{A}_{l,k})_{1,|\mathcal{I}_l|}\\ \vdots & \ddots & \vdots\\ (\mathbf{A}_{l,k})_{|\mathcal{I}_l|,1} & \cdots & (\mathbf{A}_{l,k})_{|\mathcal{I}_l|,|\mathcal{I}_l|}\end{bmatrix}, l\neq k,$$

where $(\mathbf{A}_{l,k})_{i,j}\in\mathbb{C}^{M\times M}, i,j\in 1,\cdots,|\mathcal{I}_l|$ is the block matrix of $\mathbf{A}_{l,k}$ at the ith row and jth column, given by

$$(\mathbf{A}_{l,k})_{i,j}=\begin{cases}\hat{\mathbf{h}}_{s_i^l,k}\hat{\mathbf{h}}_{s_j^l,k}^{\mathrm{H}}, & \text{if } s_i^l,s_j^l\in\mathcal{I}_k, i\neq j,\\ \hat{\mathbf{h}}_{s_i^l,k}\hat{\mathbf{h}}_{s_j^l,k}^{\mathrm{H}}+\varepsilon_{s_i^l,k}\mathbf{I}_{M\times M}, & \text{if } s_i^l,s_j^l\in\mathcal{I}_k, i=j,\\ \alpha_{s_i^l,k}\mathbf{I}_{M\times M}, & \text{if } s_i^l,s_j^l\notin\mathcal{I}_k,\ i=j,\\ \mathbf{0}_{M\times M}, & \text{otherwise}.\end{cases}$$

It can be easily verified that $\mathbf{A}_{l,k}$ is a positive definite matrix. We then plug the lower bound of the rate into the optimization problem, which can be solved efficiently.

V. Simulation Results

In this section, we evaluate the performance of the proposed algorithms. The dense C-RAN network is assumed to be deployed in a 2 km $\times$ 2 km for large C-RAN. The channel gains are composed of: 1) the path loss is modeled as $PL_{i,k}=148.1+37.6\log_{10}d_{i,k}$ (dB) [13], where $d_{i,k}$(km) is the distance; 2) the log-normal shadowing fading with zero mean and 8 dB standard derivation; 3) Rayleigh fading with zero mean and unit variance. All UEs are assumed to have the same rate requirements, i.e., $R_{\min}=R_{k,\min},\forall k$, and all fronthaul links have the same fronthaul capacity constraints, i.e., $C_{\max}=C_{i,\max},\forall i$. For ease of exposition, the normalized fronthaul capacity is considered, i.e., $\tilde{C}_{\max}=C_{\max}/R_{\min}$. It is assumed that each UE chooses its nearest L RRHs as its serving cluster, i.e., $|\mathcal{I}_k|=L,\forall k$. the other system parameters are set as follows: the number of transmit antennas at each RRH $M=2$, $K=18$, $I=30$, system bandwidth $B=20$ MHz, error tolerance $\delta=10^{-5}$, noise power spectral density is -174 dBm/Hz, each RRH's maximum power $P_{i,\max}=2$ W$,\forall i$, large constant $\Gamma=10^5$, the pilot power at each UE is $p_t=4$ W, the parameter θ in the fractional function is $\theta=10^{-5}$, the minimum rate requirement for each UE $R_{\min}=4$ bit/s/Hz, $\tilde{C}_{\max}=3$, the cluster size for each UE $L=3$, the proportion of pilots for training in one coherence time is 1% [14].

We compared our proposed algorithms (with legend "Proposed") with the following algorithms:

1) Orthogonal pilot allocation (with legend "Ortho"): In this approach, τ pilots are allocated to τ UEs that are randomly selected from K UEs.
2) No reallocation operations for Case II in Stage I (with legend "NoCaseII"): This approach is similar to the proposed pilot allocation method in Stage I, except when Case II happens, no additional operation is applied to reallocate the pilots.
3) Conventional pilot allocation method (with legend "Con"): This approach is similar to the above approach, except when Case I happens, UEs are randomly removed until the minimum number of pilots is equal to τ.
4) Perfect CSI estimation (with legend "Perfect"): In this approach, we assume that the CSI within each UE's serving cluster can be perfectly known.
5) Exhaustive search method (with legend "Exhau"): In this approach, exhaustive search method is adopted to find the maximum number of UEs that can be admitted in

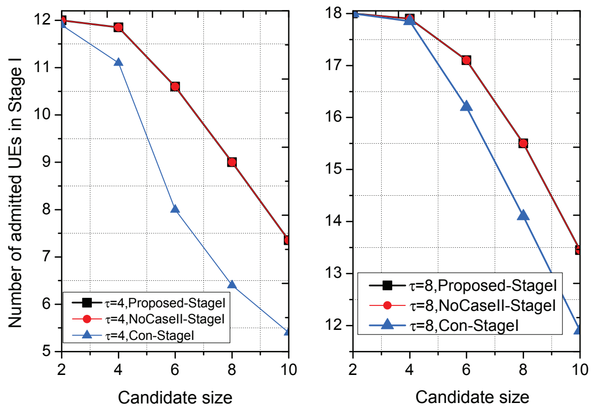

Fig. 3. Number of admitted UEs in Stage I versus the candidate size L. The left subplot corresponds to the case when the number of available pilots is $\tau = 4$ while the right one is $\tau = 8$.

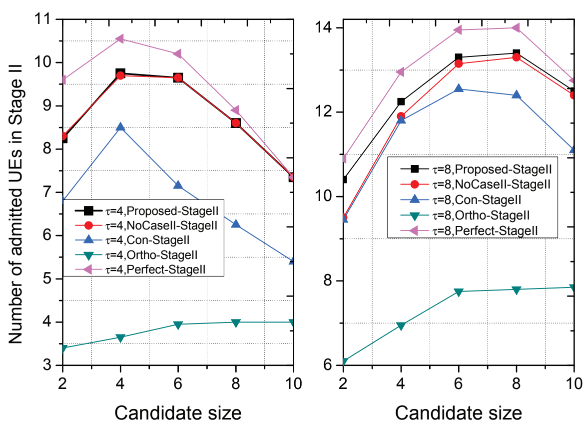

Fig. 4. Number of admitted UEs in Stage II versus the candidate size L. The left subplot corresponds to the case when the number of available pilots is $\tau = 4$ while the right one is $\tau = 8$.

Stage I. In Stage II, exhaustive search method is used to find the maximum number of admitted UEs.

Figs. 3 and 4 illustrate the number of admitted UEs versus the candidate size L in Stage I and Stage II [2], respectively. It is seen from Fig. 3 that the numbers of admitted UEs achieved by all the algorithms in Stage I decrease with the candidate size. The reason is that with the increase of candidate size, more and more UEs will be connected with each other when constructing the undirected graph. In this case, more UEs will be removed in this stage to satisfy conditions C1 and C2. Fig. 3 also shows that our proposed algorithm achieve superior performance over the "Con" algorithm, highlighting the importance of carefully considering pilot interference when removing UEs.

It is interesting to observe from Fig. 4 that the number of admitted UEs in Stage II obtained by all the algorithms (except the "Ortho" algorithm) first increase with the candidate size, and then decrease with it. The reason for the former part is due to the increased spatial degrees of freedom with the increased candidate size. However, when the candidate size becomes large, many UEs have been prohibited to be admitted due to the pilot allocation in Stage I as seen in Fig. 3. Hence, in Stage II, even all the selected UEs from Stage I can be admitted, the number is small. This trend is different from most of the existing papers [5], [7], [8], where the system performance always increases with the candidate size. This is because the pilot allocation stage was not considered in these papers. Hence, the cluster size should be properly optimized and larger cluster size may deteriorate the system performance if channel estimation process is taken into account. More interesting and insightful observations can be found in [15].

[2]The algorithm in Stage II is given in [15].

VI. Conclusions

In this paper, we considered a two-stage problem for ultra-dense C-RAN: the channel estimation for intra-cluster CSI in Stage I and robust beam-vector design in Stage II. Simulation results verify the effectiveness of the proposed algorithm in terms of the number of admitted UEs compared with the existing naive pilot allocation method. Some interesting observations have been found in the simulations. For example, increasing the cluster/candidate size may not lead to the increased performance when taking the channel estimation into account. Hence, the cluster size should be carefully decided when designing the transmission scheme.

References

[1] J. Wu, Z. Zhang, Y. Hong, and Y. Wen, "Cloud radio access network (C-RAN): a primer," *IEEE Netw.*, vol. 29, no. 1, pp. 35–41, Jan. 2015.

[2] X. Ge, S. Tu, G. Mao, C. X. Wang, and T. Han, "5G ultra-dense cellular networks," *IEEE Wireless Commun. Mag.*, vol. 23, no. 1, pp. 72–79, Feb. 2016.

[3] Y. Shi, J. Zhang, and K. Letaief, "Group sparse beamforming for green Cloud-RAN," *IEEE Trans. Wireless Commun.*, vol. 13, no. 5, pp. 2809–2823, May 2014.

[4] B. Dai and W. Yu, "Sparse beamforming and user-centric clustering for downlink cloud radio access network," *IEEE Access,*, vol. 2, pp. 1326–1339, Oct. 2014.

[5] C. Pan, H. Zhu, N. J. Gomes, and J. Wang, "Joint precoding and RRH selection for user-centric green MIMO C-RAN," *IEEE Trans. Wireless Commun.*, vol. 16, no. 5, pp. 2891–2906, May 2017.

[6] G. Caire, S. A. Ramprashad, and H. C. Papadopoulos, "Rethinking network MIMO: Cost of CSIT, performance analysis, and architecture comparisons," in *Information Theory and Applications Workshop (ITA), 2010*, 2010, pp. 1–10.

[7] C. Pan, H. Zhu, N. J. Gomes, and J. Wang, "Joint user selection and energy minimization for ultra-dense multi-channel C-RAN with incomplete CSI," *IEEE J. Sel. Areas Commun.*, vol. 35, no. 8, pp. 1809–1824, Aug. 2017.

[8] T. R. Lakshmana, A. Tolli, R. Devassy, and T. Svensson, "Precoder design with incomplete feedback for joint transmission," *IEEE Trans. Wireless Commun.*, vol. 15, no. 3, pp. 1923–1936, Mon. 2016.

[9] D. Liu, S. Han, C. Yang, and Q. Zhang, "Semi-dynamic user-specific clustering for downlink cloud radio access network," *IEEE Trans. Veh. Technol.*, vol. 65, no. 4, pp. 2063–2077, May 2016.

[10] D. Brélaz, "New methods to color the vertices of a graph," *Communications of the ACM*, vol. 22, no. 4, pp. 251–256, 1979.

[11] Z. Chen, X. Hou, and C. Yang, "Training resource allocation for user-centric base station cooperation networks," *IEEE Trans. Veh. Technol.*, vol. 65, no. 4, pp. 2729–2735, Apr. 2016.

[12] J. Jose, A. Ashikhmin, T. L. Marzetta, and S. Vishwanath, "Pilot contamination and precoding in multi-cell TDD systems," *IEEE Trans. Wireless Commun.*, vol. 10, no. 8, pp. 2640–2651, Aug. 2011.

[13] E. U. T. R. Access, "Further advancements for E-UTRA physical layer aspects," *3GPP TR 36.814, Tech. Rep.*, 2010.

[14] G. R1-074068, "Summary of reflector discussions on E-UTRA UL RS," *3GPP TSG RAN WG1 Meeting 50bis*, Oct. 2007.

[15] C. Pan and et al, "Joint pilot allocation and transmission design for ultra-dense TDD C-RAN with imperfect CSI," *To be available in Arxiv*.